Journal of the Iranian Chemical Society
https://doi.org/10.1007/s13738-020-02004-y

ORIGINAL PAPER

Synthesis, antitumor activity, enzyme assay, DNA binding and molecular docking of *Bis*-Schiff bases of pyrazoles

Nesrin M. Morsy[1] · Ashraf S. Hassan[1] · Taghrid S. Hafez[1] · Mohamed R. H. Mahran[1] · Inass A. Sadawe[2] · Abdul M. Gbaj[2]

Received: 5 May 2020 / Accepted: 11 July 2020

Abstract
A novel series of *Bis*-Schiff bases of pyrazoles **9**–**24** were synthesized by the direct condensation of 5-aminopyrazoles **4a**–**d** with dialdehydes **8a**–**d** in ethanol. The newly synthesized *Bis*-Schiff bases of pyrazoles **9**–**24** were characterized and confirmed by analytical and spectroscopic data. Some selected *Bis*-Schiff bases were investigated for their in vitro anti-proliferation activity toward three human carcinoma cell lines {HepG2 (liver), MCF-7 (breast) and RPE-1 (normal retina pigmented epithelium)} using MTT assay. The result in vitro showed that the compound **23** was found to be the active candidate against HepG2 and MCF-7 cells, while compound **16** was found to be the most potent derivative against RPE-1 cells. All the *Bis*-Schiff bases of pyrazoles **9**–**24** were evaluated for their screening on thymidine phosphorylase and DNA binding energy. The DNA binding energy showed that the compound **12** shows the lowest IC_{50} compared to other series of compounds and is the nearest one to the IC_{50} of the standard taxol. The molecular docking of the new *Bis*-Schiff base **9** was carried out and showed good binding energies (−4.45, −4.95, −2.62, −3.83 and −5.03 kcal/mol with 1bna, 102d, 1k2j, 2gvr and 2des double-strand DNA targets, respectively) when compared to standard doxorubicin. This study is an introduction to promising compounds.

Keywords *Bis*-Schiff bases · Pyrazole · Dialdehyde · Antitumor activity · DNA binding energy · Molecular docking

Introduction

A cancer disease is a malignant disease due to the uncontrolled growth of abnormal cells. Chemotherapy is a major treatment for cancer disease. Damaging of DNA protein constituents is a principle target to destroy cell's growth [1]. DNA in cancer cells could be selectively damaged, as a result of interactions with anticancer agents; consequently, blocking of cells division leads to cells death [2, 3]. The molecules that interact with DNA are generally bound to DNA through non-covalent bonds by three main mechanisms: groove binding, intercalation or static electronic interactions. Currently, it is too important to be careful about the design and synthesizing of more effective and safer human therapeutic agents to treat and overcome tumor growth.

Schiff bases exhibited wide range of medicinal applications with its azomethine (imine) functional group since this linkage is an essential feature for bioactivity. Also, Schiff bases containing heterocyclic derivatives were assigned to have different pharmacological activities like compound **A**, 1-cyclopropyl-6-fluoro-7-(4-(((*Z*)-5-fluoro-3-(4-((*E*)-4-hydroxybenzylideneamino)phenylimino)-2-oxoindolin-1-yl)methyl)piperazin-1-yl)-4-oxo-1,4-dihydroquinoline-3-carboxylic acid, which is a promising antimicrobial agent [4]. Compound **B**, 3-(3,5-dichlorobenzylideneamino)-2-methylquinazolin-4(3*H*)-one, was found to be the most potent anthelmintic agent [5]. Compound **C**, 3-(2-hydroxybenzylideneamino)-2-phenylquinazolin-4(3*H*)-one, showed better antiviral activity [6], and compounds, *N*-(2,4-dichlorobenzylidene)-4-phenyl-5-(1*H*-1,2,4-triazol-1-yl)thiazol-2-amine (**D**), *N*-(3-nitrobenzylidene)-4-phenyl-5-(1*H*-1,2,4-triazol-1-yl)thiazol-2-amine (**E**) and

✉ Ashraf S. Hassan
ashraf_salmoon@yahoo.com
https://www.scopus.com/authid/detail.uri?authorId=55318442700

[1] Organometallic and Organometalloid Chemistry Department, National Research Centre, Cairo, Dokki 12622, Egypt

[2] Department of Medicinal Chemistry, Faculty of Pharmacy, University of Tripoli, Tripoli, Libya

Published online: 22 July 2020

N-(2,4-dinitrobenzylidene)-4-phenyl-5-(1*H*-1,2,4-triazol-1-yl)thiazol-2-amine (**F**), were found to be good antitumor candidates [7].

Pyrazole is an important unit to build biologically active moieties for detection and expansion of new drugs used particularly in cancer treatment. Moreover, pyrazole moiety has important biological activities as cytotoxic, antiviral, antimicrobial and antitumor [8–11].

Schiff bases of pyrazole exhibited biological activities; compounds, 4-((3-phenyl-1*H*-pyrazol-4-yl) methyleneamino)-4*H*-1,2,4-triazole-3-thiol (**G**) and 5-ethyl-4-((3-(4-fluorophenyl)-1*H*-pyrazol-4-yl)methyleneamino)-4*H*-1,2,4-triazole-3-thiol (**H**), have exhibited significant biological activities against *Staphylococcus aureus* [12], and compound **I**, 5-((5-chloro-1-(4-fluorophenyl)-3-methyl-1*H*-pyrazol-4-yl)methyleneamino)-1-(4-(trifluoromethyl) phenyl)-1*H*-pyrazole-4-carbonitrile, showed the most potent anti-tobacco mosaic virus (TMV) [13]. *Bis*-Schiff bases also exhibited antibacterial, antifungal and antiviral activities [14] (Fig. 1).

From the above facts and in continuation to our research program for developing more promising molecules [15–35], we synthesized *Bis*-Schiff bases of pyrazoles **9**–**24** and evaluated their antitumor activity, enzyme assay, DNA binding capability and molecular docking study.

Results and discussion

Chemistry

A series of 5-aminopyrazoles **4a**–**d** was prepared as described in the literature (Scheme 1) [36, 37].

Also, dibromoalkyl **5a**, **b** {dibromomethane (**5a**) and 1,2-dibromoethane (**5b**)} were reacted with salicylaldehyde (**6**) or 4-hydroxybenzaldehyde (**7**) to yield dialdehydes **8a**, **b** {2,2′-methylene*bis*(oxy)dibenzaldehyde (**8a**) [38] and 2,2′-(ethane-1,2-diyl*bis*(oxy))dibenzaldehyde (**8b**) [39]} or **8c**, **d** {4,4′-methylene*bis*(oxy)dibenzaldehyde (**8c**) [40] and 4,4′-(ethane-1,2-diyl*bis*(oxy))dibenzaldehyde (**8d**) [40]}, respectively (Scheme 2).

The synthesized target compounds, *Bis*-Schiff bases of pyrazoles **9**–**16** and **17**–**24** were shown in Scheme 3 and were synthesized by direct condensation of 5-aminopyrazoles **4a**–**d** with dialdehydes **8a**, **b** and **8c**, **d**, respectively. (Scheme 3, Table 1).

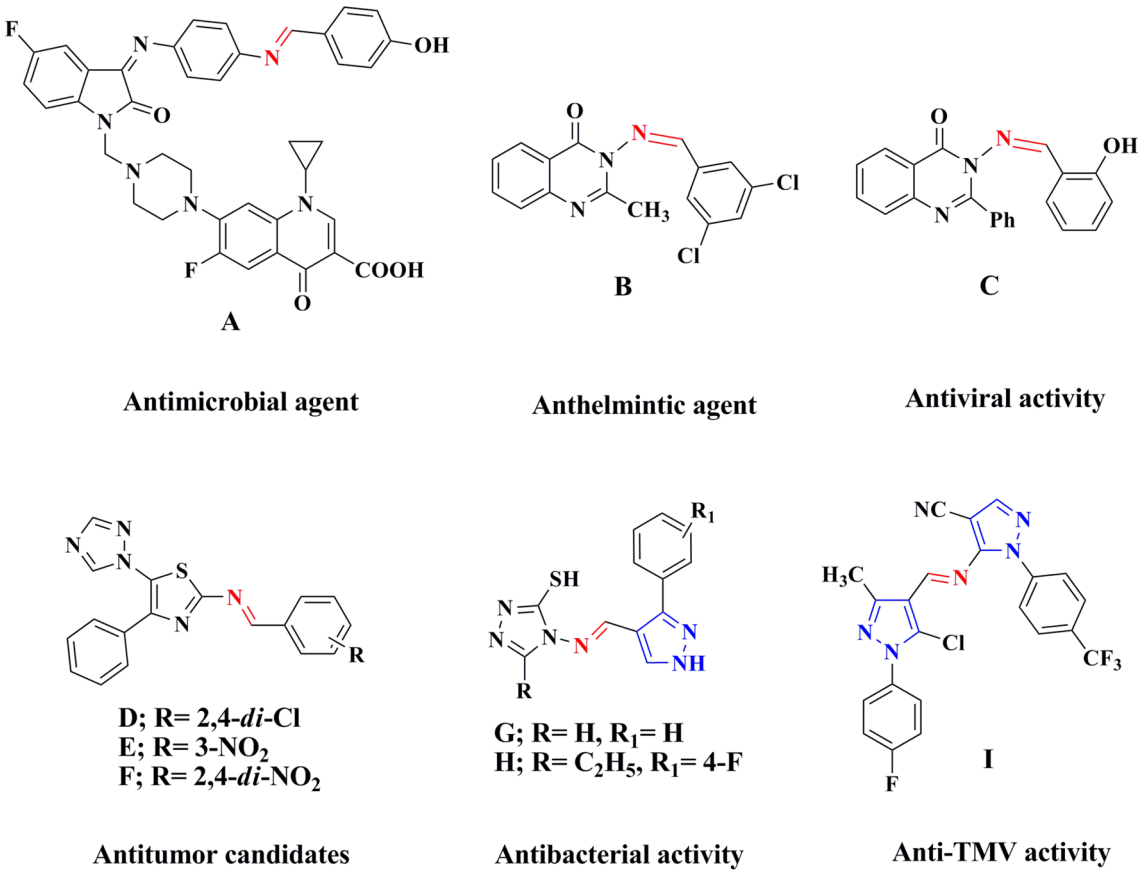

Fig. 1 Structures of the biological activities of Schiff bases **A**–**I**

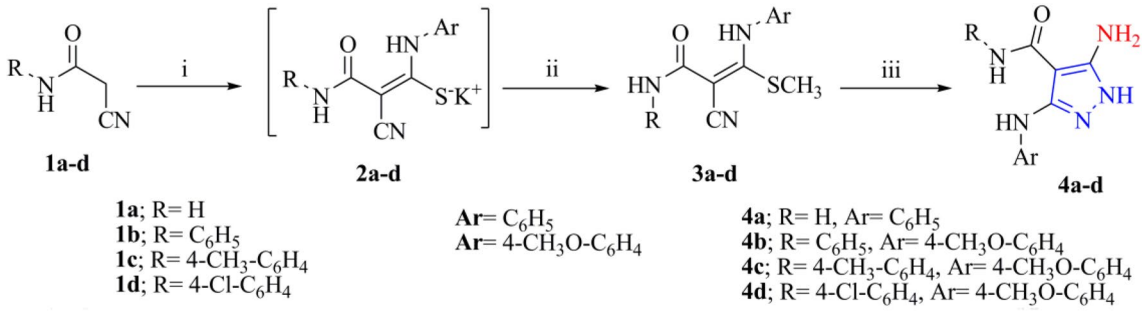

Scheme 1 Synthesis of compounds **4a–d**, reagents and conditions: (1) Ar = Ph–NCS or 4–CH_3O–C_6H_4–NCS/KOH/EtOH. (2) CH_3I/EtOH/r.t. (3) NH_2NH_2/TEA/EtOH/reflux 4 h

Scheme 2 Synthesis of dialdehydes **8a**, **b** and **8c**, **d**

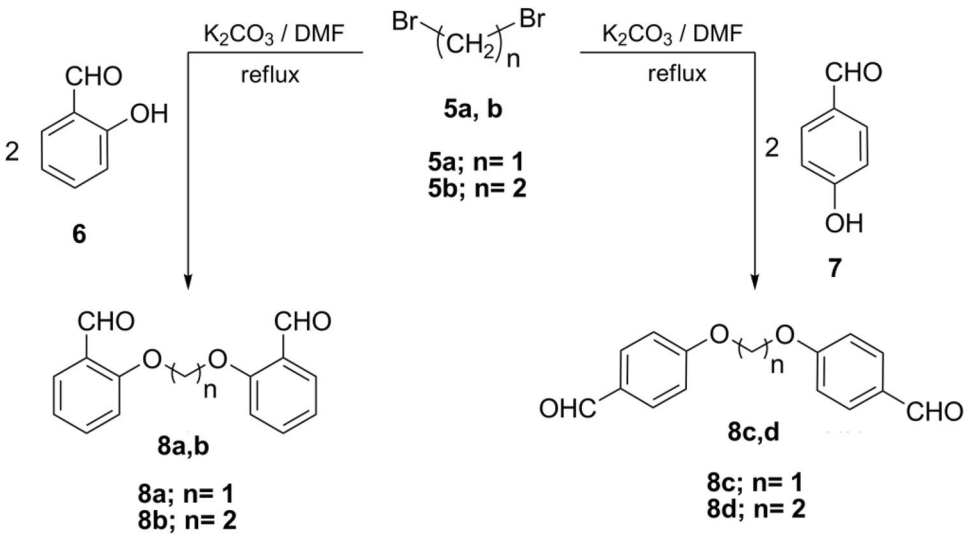

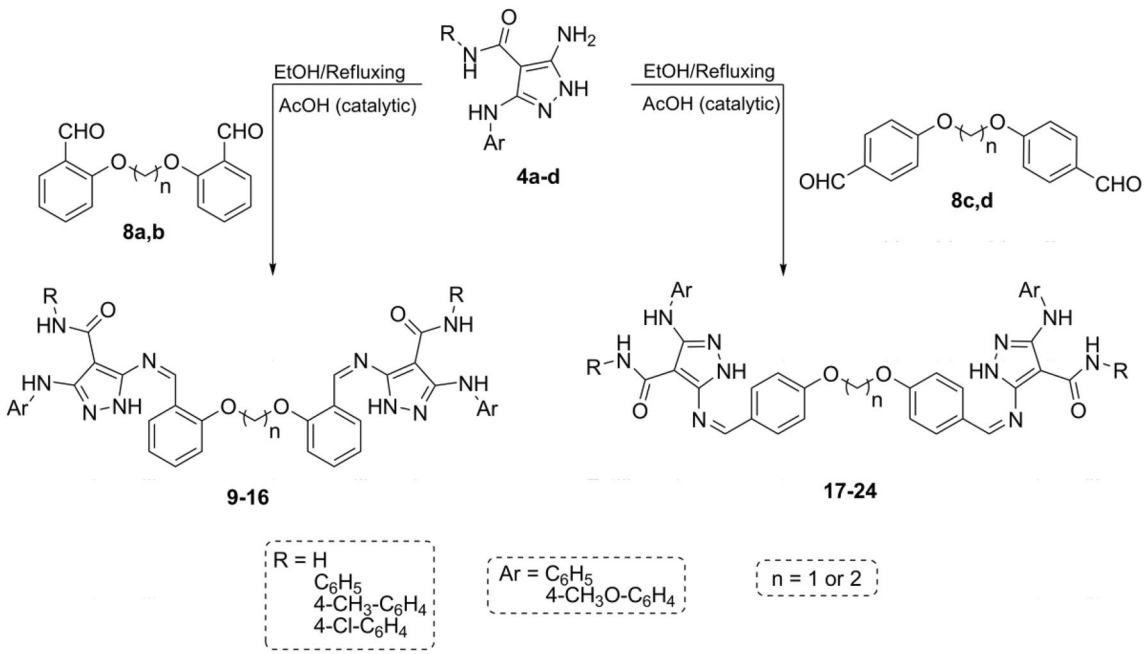

Scheme 3 Synthesis of *Bis*-Schiff bases **9–24**

Table 1 *Bis*-Schiff bases **9**–**24**

Compounds	*n*	R	Ar
9	1	H	Ph
10	1	Ph	4–CH_3O–C_6H_4
11	1	4–CH_3–C_6H_4	4–CH_3O–C_6H_4
12	1	4–Cl–C_6H_4	4–CH_3O–C_6H_4
13	2	H	Ph
14	2	Ph	4–CH_3O–C_6H_4
15	2	4–CH_3–C_6H_4	4–CH_3O–C_6H_4
16	2	4–Cl–C_6H_4	4–CH_3O–C_6H_4
17	1	H	Ph
18	1	Ph	4–CH_3O–C_6H_4
19	1	4–CH_3–C_6H_4	4–CH_3O–C_6H_4
20	1	4–Cl–C_6H_4	4–CH_3O–C_6H_4
21	2	H	Ph
22	2	Ph	4–CH_3O–C_6H_4
23	2	4–CH_3–C_6H_4	4–CH_3O–C_6H_4
24	2	4–Cl–C_6H_4	4–CH_3O–C_6H_4

The structures of the *Bis*-Schiff bases of pyrazoles **9**–**16** and **17**–**24** were established and confirmed on the basis of their elemental analysis and spectral data. For example, structure **24**, 5,5′-(4,4′-ethylenebis(oxy)*bis*(benzylideneamino))*bis*(3-(4-methoxyphenylamino)-*N*-(4-chlorophenyl)-1*H*-pyrazole-4-carboxamide), was supported by its mass (949.84), which agrees with its molecular formula $C_{50}H_{42}Cl_2N_{10}O_6$; its IR (KBr) ν_{max}/cm^{-1} spectrum showed 3426, 3272 for NH function and 1656 for C=O group; its ^{1}H NMR (DMSO-d_6, δ ppm) spectrum showed two signals at 4.50 (4*H*) and 8.66 (2*H*) corresponding to two CH_2 and two –N=CH– groups, respectively. Also, the ^{1}H NMR spectrum showed the following: 3.72 (6H, s, 2OCH_3), 6.90 (4H, *d*, *J* = 8.1 Hz, ArH), 7.18–7.26 (6H, *m*, ArH), 7.41 (4H, *d*, *J* = 8.6 Hz, ArH), 7.69 (4H, *d*, *J* = 8.6 Hz, ArH), 7.88 (2H, *d*, *J* = 8.6 Hz, ArH), 8.04 (4H, *d*, *J* = 8.2 Hz, ArH), 8.96 (2H, *s*, 2NH), 9.88 (2H, *s*, 2NH), 12.63 (2H, *s*, 2NH). Its ^{13}C NMR spectrum (DMSO-d_6, δ ppm) was characterized by signals at 66.71 and 156.52 assigned to CH_2 and –N=CH– groups, respectively. Moreover, the ^{13}C NMR showed 55.24 (2C, 2OCH_3), 93.51 (2C_4, pyrazole), 114.41, 115.47, 120.57, 128.92, 129.88, 131.42, 133.24, 137.50, 151.86 (34C, Ar), 153.10 (2C_5, pyrazole), 155.27 (2C_3, pyrazole), 162.33 (2C, Ar), 162.83 (2C=O).

Biological evaluation

Cytotoxicity activity

Selected eight *Bis*-Schiff bases of pyrazoles were examined in vitro for their cytotoxicity against HepG2 (human liver carcinoma), MCF-7 (human breast adenocarcinoma) and RPE-1 (human normal retina pigmented epithelium) using MTT assay [41–44]. The percentage and activities of the intact cells were measured and compared to the control (Table 2, Fig. 2). The activities of the *Bis*-Schiff bases of pyrazoles against the three human cells were compared with that of *Doxorubicin*®.

From Table 1 and Fig. 2, we can deduce that, among the derivatives, compound **23** was found to be the active candidate against HepG2 and MCF-7 cells, while compound **16** was found to be the most potent derivative against RPE-1 cells.

Thymidine phosphorylase

Thymidine phosphorylase enzyme TP has a great focusing as a cancer goal as it plays a function in tumor angiogenesis, and is observed at higher levels in the plasma of patients having cancer and in solid tumors compared to healthy tissues. Inhibitors of TP inhibit angiogenesis and metastasis as well as promoting apoptosis. Inhibitors of TP also potentiate the actions of anticancer.

No compound had any inhibition on thymidine phosphorylase enzyme as the compounds were not designed for this target.

DNA binding properties

The fluorescence intensity of DNA-bound EB at 612 nm decreased outstandingly with the increase in these compounds concentrations. This decrease perhaps is attributed to the quenching of some EB molecules that were permeated from DNA into the substituted solution by the products. The summarized IC_{50} was indicated in the attached table (Table 3).

Compound **12** shows the lowest IC_{50} compared to other series of compounds and is the nearest one to the IC_{50} of the standard taxol.

Molecular docking analysis

Table 4 shows the binding energies of our compounds and DNAs fragments obtained by the molecular docking strategy. The study of our compounds with five B-DNA fragments was achieved using AutoDock 4.2 to investigate the way of interaction forces between our compounds and DNA. The synthesized compounds and DNA were kept as flexible molecules and were docked into five forms of rigid B-DNA fragments to obtain the preferential binding site to the series of compounds on B-DNAs. The molecular docking results are shown in Table 4. The modeling studies showed that there are *van der Waals*, hydrogen bonding and electrostatic interactions between the compounds and DNAs. The sum of the first two interactions and desolvation free energy is much

Table 2 The cytotoxicity IC_{50} (μM) values of selected eight *Bis*-Schiff bases of pyrazoles using MTT assay against three human cancer cell lines types (HepG2, MCF-7 and RPE-1)

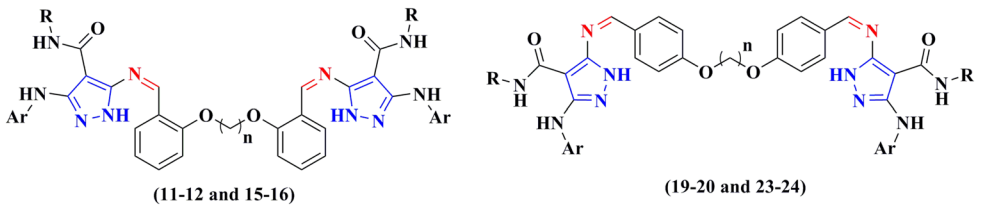

Compounds	*n*	R	Ar	IC_{50} (μM)		
				HepG2	MCF-7	RPE-1
11	1	4–CH_3–C_6H_4	4–CH_3O–C_6H_4	111.6	125.1	143.7
12	1	4–Cl–C_6H_4	4–CH_3O–C_6H_4	108.4	136.7	148.5
15	2	4–CH_3–C_6H_4	4–CH_3O–C_6H_4	100.5	125.3	143.1
16	2	4–Cl–C_6H_4	4–CH_3O–C_6H_4	88.4	107.9	127.7
19	1	4–CH_3–C_6H_4	4–CH_3O–C_6H_4	90.8	117.9	132.2
20	1	4–Cl–C_6H_4	4–CH_3O–C_6H_4	89.8	106.5	137.1
23	2	4–CH_3–C_6H_4	4–CH_3O–C_6H_4	84.2	99.4	138.2
24	2	4–Cl–C_6H_4	4–CH_3O–C_6H_4	86.2	100.7	137.2
Doxorubicin	–	–	–	25.3	20.9	19.1

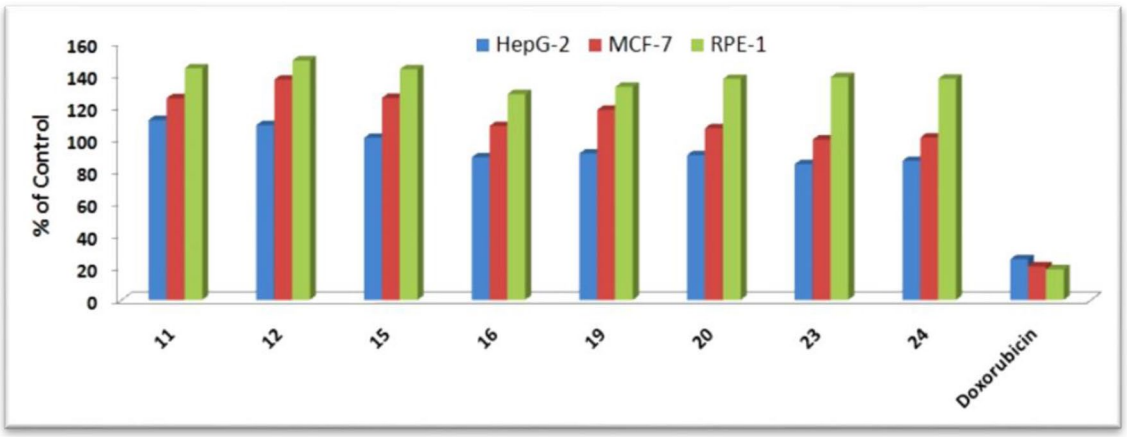

Fig. 2 Antitumor activity of the selected eight *Bis*-Schiff bases of pyrazoles against HepG2, MCF-7 and RPE-1 cell lines using MTT assay

greater than the last interaction since the contributions of the three top energies together are larger than the electrostatic energy [45, 46].

Some of the binding energies obtained by performing molecular docking simulation of the compounds with the five DNA fragments did not lie in the predefined range of − 5 kcal/mol to − 15 kcal/mol (Table 4). The obtained binding energy results demonstrate that the affinity of compounds for their "preferred" sites is modulated by the local DNA sequence. In some cases, this effect is relatively small, while in other cases, as in **9**, **13** and **19** the effect is good. Since these sequence effects lie outside the principal binding sites for these ligands, they may reflect changes in the local DNA structure and/or dynamics. This is similar to those seen in protein–DNA interactions [47, 48].

Molecular docking is used for virtual screening of our compounds employing binding affinity and the best orientation possible with respect to the target DNA to illustrate the DNA (**9**–**24**) compounds interactions; compound **9** as an example from the series was chosen and done. DNA interactions with compound **9** are shown in Fig. 3. Compound **9** showed good binding energies (− 4.45, − 4.95, − 2.62,

Table 3 DNA binding (IC_{50} (μM)) of *Bis*-Schiff bases of pyrazoles **9–24**

Compounds	IC_{50} (μM)	Compounds	IC_{50} (μM)
9	55.3 ± 3.32	**18**	70.2 ± 2.22
10	60.3 ± 2.32	**19**	72.2 ± 1.32
11	72.4 ± 3.32	**20**	55.3 ± 1.32
12	52.3 ± 1.42	**21**	72.4 ± 2.32
13	55.3 ± 2.12	**22**	79.3 ± 1.92
14	62.2 ± 2.12	**23**	80.4 ± 3.42
15	73.3 ± 2.22	**24**	60.3 ± 2.61
16	53.2 ± 2.12	Taxol	35.0 ± 1.12
17	63.3 ± 2.12		

− 3.83 and − 5.03 kcal/mol with 1bna, 102d, 1k2j, 2gvr and 2des double-strand DNA targets, respectively) when compared to standard doxorubicin as mentioned in Table 4. Double-helical structure of 1bna, 102d, 1k2j, 2gvr and 2des hydrogen bounded to the compound **9** at the minor groove is shown in Fig. 3.

The results showed that the binding energies of the Bis-Schiff bases of pyrazole **9–24** and DNAs fragments obtained by the molecular docking strategy. In this study, molecular dockings of the Bis-Schiff bases of pyrazole with three B-DNA fragments were performed using AutoDock 4.2 to investigate the binding mode of Bis-Schiff bases with B-DNA and to obtain information about interaction forces between synthesized compounds and DNA. The synthesized compounds and DNA were kept as flexible molecules and were docked into seven forms of rigid B-DNA fragments to obtain the preferential binding site to synthesized compounds on B-DNAs. The modeling studies showed that there are *van der Waals*, hydrogen bonding and electrostatic interactions between compound **9** ligand and DNAs. This fact is clear in the modeling studies of compound **9** ligand and is consistent with the literature [49, 50].

All *Bis*-Schiff bases of pyrazole **9–24** were bound to the minor groove of the three DNA fragments. This binding often has cytotoxic activity because they interfere with the binding of proteins necessary for DNA replication and transcription. In the literature, compounds that bind to the minor groove of DNA have proven to be very useful as antitumor agents because they selectively kill rapidly dividing cells [49, 51]. This has encouraged efforts to design molecules that bind at designated sites in the minor groove. It is contemplation that groove binders with increased selectivity will produce a greater biological response for a given dose and consequently have fewer

Table 4 Various energies in the binding process of Schiff bases of pyrazole **9–24** with DNAs obtained from molecular docking. The unit of all energies (ΔG) is kcal/mol

Compounds	1bna DNA (5′-D(*CP*GP*CP*GP*AP*AP*TP*TP*CP*GP*CP*G)-3′)	102d DNA (5′-D(*CP*GP*CP*AP*AP*AP*TP*TP*TP*GP*CP*G)-3′)	1k2j 5′-D(*CP*GP*TP*AP*CP*G)-3′	2gvr 5′-D(*CP*GP*CP*GP*AP*AP*TP*TP*CP*GP*CP*G)-3′	2des DNA (5′-D(*CP*GP*TP*AP*CP*G)-3′)
ΔG	Binding energy	Binding energy	Binding energy	Binding energy	Binding energy
Doxorubicin	− 7.64	− 8.41	− 6.32	− 7.64	− 4.85
9	− 4.45	− 4.95	− 2.62	− 3.83	− 5.03
10	− 3.28	− 4.13	+ 4.11	− 3.14	− 2.39
11	− 3.61	− 1.7	+ 3.23	− 0.35	− 0.49
12	− 0.47	− 0.99	+ 18.66	+ 1.27	+ 2.2
13	− 4.13	− 4.31	− 2.93	− 2.79	− 0.35
14	− 2.55	− 2.8	+ 13.09	− 1.76	− 1.84
15	− 0.52	− 0.07	+ 3.38	+ 0.23	+ 0.53
16	− 2.18	− 2.74	+ 95.28	− 0.25	+ 2.08
17	− 3.59	− 4.35	− 4.42	− 4.15	+ 1.05
18	− 1.82	− 2.52	+ 1.43	− 0.84	− 1.52
19	− 2.26	− 1.98	− 1.93	− 1.67	− 0.18
20	− 2.04	− 1.81	+ 6.11	− 2.94	+ 1.62
21	− 3.81	− 3.62	− 2.99	− 2.76	+ 1.21
22	− 1.38	− 2.14	− 0.88	− 2.38	− 1.88
23	− 2.41	− 1.25	+ 5.1	+ 0.18	+ 1.53
24	+ 1.04	− 2.92	+ 4.11	− 1.1	+ 2.03

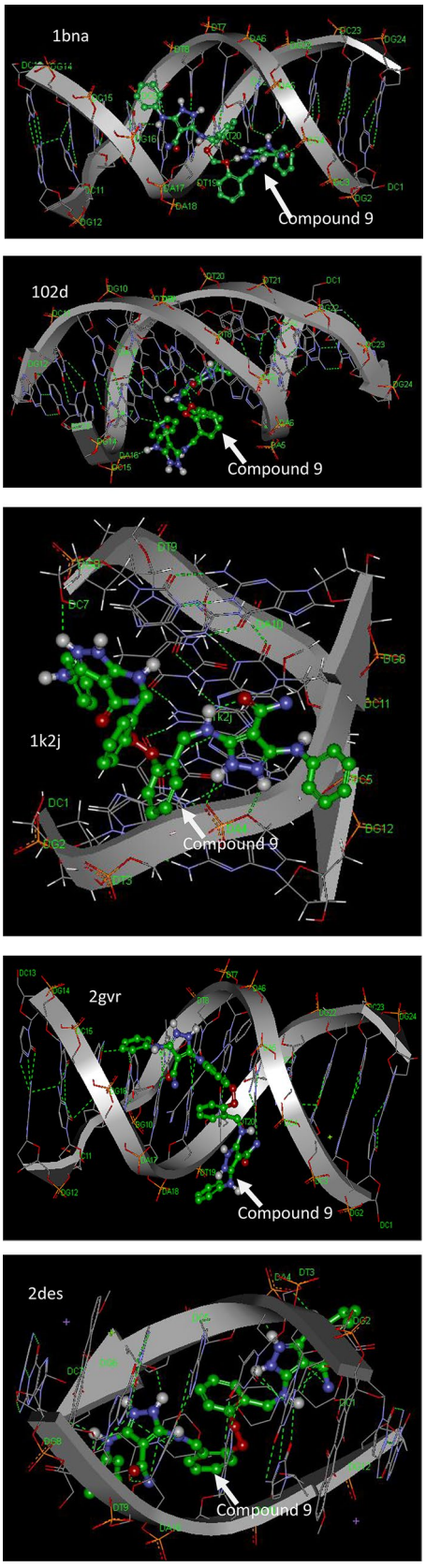

Fig. 3 Double-helical structure of 1bna, 102d, 1k2j, 2gvr and 2des hydrogen bounded to the compound **9** at the minor groove

toxic and side effects than non-selective groove binders [52].

Conclusion

In summary, we have synthesized a novel series of *Bis*-Schiff bases of pyrazoles **9**–**16** and **17**–**24** by the direct condensation of 5-aminopyrazoles **4a**–**d** with dialdehydes **8a**, **b** and **8c**, **d**, respectively, in refluxing ethanol with very high yields for evaluation of their antitumor activities against three human carcinoma cell lines (HepG2, MCF-7 and RPE-1) using MTT assay. Most of *Bis*-Schiff bases of pyrazoles displayed moderate antitumor activity. The molecular docking study of the *Bis*-Schiff base of pyrazole with B-DNA was performed. There are three modes of interaction. The modeling studies showed that the contribution of the sum of *van der Waals* and hydrogen bonding interaction is much greater than that of the electrostatic interaction. Compound **9** showed good binding energies when compared to the standard doxorubicin due to the sum of three interactions between a ligand and DNAs. Accordingly, this class of *Bis*-Schiff bases of pyrazoles **9**–**24** could be considered as useful templates for future development in derivatizations or modifications to obtain more potent and selective antitumor agents.

Experimental

Chemistry

All melting points were measured on a Gallenkamp melting point apparatus and are uncorrected. ^{1}H NMR (400 MHz) and ^{13}C NMR (100 MHz) spectra were recorded on a Varian spectrometer using DMSO-d_6 as solvent and TMS as an internal standard. Chemical shifts are reported in ppm. Coupling constants (*J*) are expressed in Hz. Mass spectra were recorded on a Varian MAT 112 spectrometer at 70 eV. Elemental analyses were performed at the Microanalytical Center, Cairo University, Egypt.

Progress of the reactions was monitored by thin-layer chromatography (TLC) using aluminum sheets coated with silica gel F_{254} (Merck), viewing under a short-wavelength UV lamp effected detection. All evaporations were carried out under reduced pressure at 40 °C.

Synthesis of 5-amino-3-(arylamino)-1H-pyrazole-4-carboxamides 4a–d

Compounds of this series were prepared according to the literature procedure:

5-Amino-3-anilino-lH-pyrazole-4-carboxamide (4a) m.p. 178–180 °C [36].
5-Amino-3-(4-methoxyphenylamino)-N-phenyl-1H-pyrazole-4-carboxamide (4b) m.p. 175–177 °C [37].
5-Amino-3-(4-methoxyphenylamino)-N-(4-methylphenyl)-1H-pyrazole-4-carboxamide (4c) m.p. 198–200 °C [37].
5-Amino-3-(4-methoxyphenylamino)-N-(4-chlorophenyl)-1H-pyrazole-4-carboxamide (4d) m.p. 190–192 °C [37].

Synthesis of dialdehydes 8a–d

To a solution of salicylaldehyde (**6**) or 4-hydroxybenzaldehyde (**7**) (0.2 mol) and K_2CO_3 (0.2 mol) in DMF (100 ml), dibromoalkyl derivatives **5a**, **b** (0.1 mol) {dibromomethane (**5a**) or 1,2-dibromoethane (**5b**)} were added dropwise. The reaction mixture was allowed to stir for 10 h at 150–155 °C and then 5 h at room temperature. After the addition was completed, then 200 ml distilled water was added and was placed in refrigerator. Then, after 1 h the solid product was filtered off, washed with ethanol, dried and finally recrystallized from DMF/H_2O to afford the corresponding dialdehydes **8a–d**:

2,2′-Methylenebis(oxy)dibenzaldehyde (8a) m.p. 132 °C [38].
2,2′-(Ethane-1,2-diylbis(oxy))dibenzaldehyde (8b) m.p. 122 °C [39].
4,4′-Methylenebis(oxy)dibenzaldehyde (8c) m.p. 215–216 [40].
4,4′-(Ethane-1,2-diylbis(oxy))dibenzaldehyde (8d) m.p. 210–212 [40].

Synthesis of Bis-Schiff bases 9–24

A reaction mixture of compounds **4a–d** (0.02 mol) and dialdehydes **8a–d** (0.01 mol) {namely 2,2′-methylenebis(oxy) dibenzaldehyde (**8a**), 2,2′-(ethane-1,2-diylbis(oxy))dibenzaldehyde (**8b**), 4,4′-methylenebis(oxy)dibenzaldehyde (**8c**) and 4,4′-(ethane-1,2-diylbis(oxy))dibenzaldehyde (**8d**)} with a catalytic amount of glacial acetic acid (1 ml) in absolute ethanol (25 ml) was refluxed for 1 h and then left to cool. The solid product was filtered off, dried and finally recrystallized from ethanol to afford the corresponding *Bis*-Schiff bases **9–24**.

5,5′-(2,2′-Methylenebis(oxy)*bis*(benzylideneamino))*bis*(3-(phenylamino)-1*H*-pyrazole-4-carboxamide) (9) Yellow crystals, m.p. 270 °C, yield (82%). IR (KBr) ν_{max}/cm^{-1} 3370 (NH), 1653 (C=O). ^{1}H NMR (DMSO-d_6, 400 MHz, δ ppm) 6.18 (2H, *s*, CH_2), 6.87 (2H, *t*, ArH), 7.20 (2H, *t*, ArH), 7.28 (4H, *t*, ArH), 7.36–7.39 (4H, *m*, ArH), 7.48 (4H, *s*, $2NH_2$), 7.57 (2H, *d*, $J=8.3$ Hz, ArH), 7.63 (2H, *d*, $J=6.8$ Hz, ArH), 8.07 (2H, d, $J=7.0$ Hz, ArH), 9.11 (2H, *s*, 2-N=CH-), 9.25 (2H, *s*, 2NH), 12.73 (2H, *s*, 2NH). ^{13}C NMR (DMSO-d_6, 75 MHz, δ ppm) 90.57 (1C, CH_2), 93.49 (2C, C_4-pyrazole), 115.44, 116.14, 120.14, 122.78, 123.67, 127.78, 128.83, 129.16, 134.78, 141.07 (22C, Ar), 153.71 (4C, C_5 and C_3, pyrazole), 156.90 (2C, 2–N=CH–), 162.19 (2C, Ar), 166.35 (2C=O). Anal. Calcd. (%) for $C_{35}H_{30}N_{10}O_4$ (654.68): C, 64.21; H, 4.62; N, 21.39. Found: C, 64.30; H, 4.55; N, 21.30%.

5,5′-(2,2′-Methylenebis(oxy)*bis*(benzylideneamino))*bis*(3-(4-methoxyphenylamino)-*N*-phenyl-1*H*-pyrazole-4-carboxamide) (10) Yellow crystals, m.p. 246 °C, yield (80%). IR (KBr) ν_{max}/cm^{-1} 3427, 3301 (NH), 1657 (C=O). ^{1}H NMR (DMSO-d_6, 400 MHz, δ ppm) 3.74 (6H, *s*, $2OCH_3$), 6.20 (2H, *s*, CH_2), 6.91 (4H, *d*, $J=8.4$ Hz, ArH), 7.03 (2H, *t*, ArH), 7.29–7.40 (10H, *m*, ArH), 7.57–7.69 (8H, *m*, ArH), 8.16 (2H, *d*, $J=7.5$ Hz, ArH), 8.69 (2H, *s*, 2–N=CH–), 9.33 (2H, *s*, 2NH), 9.92 (2H, *s*, 2NH), 12.27 (2H, *s*, 2NH). ^{13}C NMR (DMSO-d_6, 100 MHz, δ ppm) 55.28 (2C, $2OCH_3$), 91.16 (3C, $1CH_2$ and $2C_4$-pyrazole), 114.49, 115.94, 118.98, 123.27, 124.30, 127.02, 129.01, 134.82, 138.51, 149.88 (34C, Ar), 152.85 ($2C_5$, pyrazole), 154.61 ($2C_3$, pyrazole), 157.12 (2C, 2–N=CH–), 161.15 (2C, Ar), 162.71 (2C=O). Anal. Calcd. (%) for $C_{49}H_{42}N_{10}O_6$ (866.92): C, 67.89; H, 4.88; N, 16.16. Found: C, 68.00; H, 4.80; N, 16.20%.

5,5′-(2,2′-Methylenebis(oxy)*bis*(benzylideneamino))*bis*(3-(4-methoxyphenylamino)-*N*-(4-methylphenyl)-1*H*-pyrazole-4-carboxamide) (11) Yellow crystals, m.p. 268 °C, yield (82%). IR (KBr) ν_{max}/cm^{-1} 3427, 3285 (NH), 1651 (C=O). ^{1}H NMR (DMSO-d_6, 400 MHz, δ ppm) 2.22 (6H, *s*, $2CH_3$), 3.73 (6H, *s*, $2OCH_3$), 6.19 (2H, *s*, CH_2), 6.91 (4H, *d*, $J=8.1$ Hz, ArH), 7.09 (4H, *d*, $J=7.9$ Hz, ArH), 7.26–7.68 (14H, *m*, ArH), 8.11 (2H, *d*, $J=7.2$ Hz, ArH), 8.70 (2H, *s*, 2–N=CH–), 9.28 (2H, *s*, 2NH), 9.82 (2H, *s*, 2NH), 12.69 (2H, *s*, 2NH). ^{13}C NMR (DMSO-d_6, 75 MHz, δ ppm) 20.37 (2C, $2CH_3$), 55.20 (2C, $2OCH_3$), 90.64 (2C, CH_2), 91.09 (2C, C_4-pyrazole), 114.39, 115.96, 117.55, 119.76, 122.66, 123.20, 124.30, 127.85, 129.31, 132.05, 134.81, 135.92, 136.30 (31C, Ar), 154.13 (4C, C_5 and C_3 pyrazole), 155.58 (2C, Ar), 157.02 (2C, 2–N=CH–), 162.48 (2C, Ar), 165.16 (2C=O). Anal. Calcd. (%) for $C_{51}H_{46}N_{10}O_6$ (894.97): C, 68.44; H, 5.18; N, 15.65. Found: C, 68.50; H, 5.10; N, 15.70%.

5,5′-(2,2′-Methylene*bis*(oxy)*bis*(benzylideneamino))*bis*(3-(4-methoxyphenylamino)-*N*-(4-chlorophenyl)-1*H*-pyrazole-4-carboxamide) (12) Yellow crystals, m.p. 262 °C, yield (80%). IR (KBr) ν_{max}/cm^{-1} 3436 (NH), 1655 (C=O). ^{1}H NMR (DMSO-d_6, 400 MHz, δ ppm) 3.73 (6H, *s*, $2OCH_3$), 6.19 (2H, *s*, CH_2), 6.89 (4H, *d*, *J* = 8.9 Hz, ArH), 7.25–7.37 (10H, *m*, ArH), 7.56–7.68 (8H, *m*, ArH), 8.09 (2H, *d*, *J* = 6.7 Hz, ArH), 8.61 (2H, *s*, 2–N=CH–), 9.25 (2H, *s*, 2NH), 9.94 (2H, *s*, 2NH), 12.30 (2H, *s*, 2NH). Anal. Calcd. (%) for $C_{49}H_{40}Cl_2N_{10}O_6$ (935.81): C, 62.89; H, 4.31; N, 14.97. Found: C, 62.80; H, 4.35; N, 15.00%.

5,5′-(2,2′-Ethylenebis(oxy)*bis*(benzylideneamino))*bis*(3-(phenylamino)-1*H*-pyrazole-4-carboxamide) (13) Yellow crystals, m.p. 258 °C, yield (79%). ^{1}H NMR (DMSO-d_6, 400 MHz, δ ppm) 4.62 (4H, *s*, $2CH_2$), 6.84 (2H, *t*, ArH), 7.08 (2H, *t*, ArH), 7.26 (6H, *t*, ArH), 7.33 (4H, *d*, *J* = 7.8 Hz, ArH), 7.45 (4H, *d*, $2NH_2$), 7.57 (2H, *t*, ArH), 8.02 (2H, *d*, *J* = 7.3 Hz, ArH), 9.08 (2H, *s*, 2 N = CH-), 9.19 (2H, *s*, 2NH), 12.12 (2H, *s*, 2NH). ^{13}C NMR (DMSO-d_6, 100 MHz, δ ppm) 68.26 (2C, $2CH_2$), 93.86 ($2C_4$, pyrazole), 114.28, 116.85, 121.90, 123.79, 127.90, 129.51, 130.10, 135.14, 141.68 (22C, Ar), 152.17 ($2C_5$, pyrazole), 154.06 ($2C_3$, pyrazole), 159.77 (2C, 2–N=CH–), 163.96 (2C, Ar), 166.76 (2C=O). Anal. Calcd. (%) for $C_{36}H_{32}N_{10}O_4$ (668.70): C, 64.66; H, 4.82; N, 20.95. Found: C, 64.60; H, 4.90; N, 21.00%.

5,5′-(2,2′-Ethylenebis(oxy)*bis*(benzylideneamino))*bis*(3-(4-methoxyphenylamino)-*N*-phenyl-1*H*-pyrazole-4-carboxamide) (14) Orange crystals, m.p. 256 °C, yield (83%). IR (KBr) ν_{max}/cm^{-1} 3281 (NH), 1655 (C=O). ^{1}H NMR (DMSO-d_6, 400 MHz, δ ppm) 3.70 (6H, *s*, $2OCH_3$), 4.61 (4H, *s*, $2CH_2$), 6.84 (4H, *d*, *J* = 8.9 Hz, ArH), 7.05 (2H, *t*, ArH), 7.20 (2H, *t*, ArH), 7.31–7.36 (10H, *m*, ArH), 7.61 (6H, *d*, *J* = 7.8 Hz, ArH), 8.15 (2H, *d*, *J* = 7.7 Hz, ArH), 8.65 (2H, *s*, 2–N=CH–), 9.36 (2H, *s*, 2NH), 9.98 (2H, *s*, 2NH), 12.83 (2H, *s*, 2NH). Anal. Calcd. (%) for $C_{50}H_{44}N_{10}O_6$ (880.95): C, 68.17; H, 5.03; N, 15.90. Found: C, 68.20; H, 5.00; N, 15.85%.

5,5′-(2,2′-Ethylenebis(oxy)*bis*(benzylideneamino))*bis*(3-(4-methoxyphenylamino)-*N*-(4-methylphenyl)-1*H*-pyrazole-4-carboxamide) (11) Yellow crystals, m.p. > 300 °C, yield (75%). IR (KBr) ν_{max}/cm^{-1} 3426, 3277 (NH), 1653 (C=O). ^{1}H NMR (DMSO-d_6, 400 MHz, δ ppm) 2.25 (6H, *s*, $2CH_3$), 3.70 (6H, *s*, $2OCH_3$), 4.61 (4H, *s*, $2CH_2$), 6.84 (4H, *d*, *J* = 8.7 Hz, ArH), 7.12 (4H, *d*, *J* = 8.0 Hz, ArH), 7.19 (2H, *t*, ArH), 7.34 (6H, *d*, *J* = 8.1 Hz, ArH), 7.49 (4H, *d*, *J* = 8.1 Hz, ArH), 7.62 (2H, *t*, ArH), 8.12 (2H, *d*, *J* = 7.4 Hz, ArH), 8.67 (2H, *s*, 2–N=CH–), 9.33 (2H, *s*, 2NH), 9.90 (2H, *s*, 2NH), 12.29 (2H, *s*, 2NH). ^{13}C NMR (DMSO-d_6, 100 MHz, δ ppm) 20.42 (2C, $2CH_3$), 55.21 (2C, $2OCH_3$), 67.84 (2C, $2CH_2$), 89.81 ($2C_4$, pyrazole), 113.78, 114.40, 115.46, 121.63, 123.51, 126.77, 129.39, 132.05, 134.78, 136.08, 151.18 (34C, Ar), 153.35 ($2C_5$, pyrazole), 155.47 ($2C_3$, pyrazole), 156.66 (2C, 2–N=CH–), 159.49 (2C, Ar), 162.60 (2C=O). Anal. Calcd. (%) for $C_{52}H_{48}N_{10}O_6$ (909.00): C, 68.71; H, 5.32; N, 15.41. Found: C, 68.80; H, 5.25; N, 15.47%.

5,5′-(2,2′-Ethylenebis(oxy)*bis*(benzylideneamino))*bis*(3-(4-methoxyphenylamino)-*N*-(4-chlorophenyl)-1*H*-pyrazole-4-carboxamide) (16) Orange crystals, m.p. 270 °C, yield (75%). IR (KBr) ν_{max}/cm^{-1} 3429, 3277 (NH), 1657 (C=O). ^{1}H NMR (DMSO-d_6, 400 MHz, δ ppm): 3.69 (6H, *s*, $2OCH_3$), 4.60 (4H, *s*, $2CH_2$), 6.79 (4H, *d*, *J* = 8.7 Hz, ArH), 7.17–7.35 (12H, *m*, ArH), 7.57–7.64 (6H, *m*, ArH), 8.10 (2H, *d*, *J* = 7.3 Hz, ArH), 8.59 (2H, *s*, 2–N=CH–), 9.32 (2H, *s*, 2NH), 9.98 (2H, *s*, 2NH), 12.42 (2H, *s*, 2NH). ^{13}C NMR (DMSO-d_6, 100 MHz, δ ppm) 55.17 (2C, $2OCH_3$), 67.97 (2C, $2CH_2$), 92.86 ($2C_4$, pyrazole), 114.29, 118.15, 120.41, 121.72, 123.58, 124.99, 126.48, 126.82, 128.74, 132.92, 134.77, 137.50, 148.11 (34C, Ar), 152.54 ($2C_5$, pyrazole), 157.11 ($2C_3$, pyrazole), 159.58 (2C, 2–N=CH–), 162.09 (2C, Ar), 162.67 (2C=O). Anal. Calcd. (%) for $C_{50}H_{42}Cl_2N_{10}O_6$ (949.84): C, 63.23; H, 4.46; N, 14.75. Found: C, 63.30; H, 4.39; N, 14.80%.

5,5′-(4,4′-Methylenebis(oxy)*bis*(benzylideneamino))*bis*(3-(phenylamino)-1*H*-pyrazole-4-carboxamide) (17) Yellow crystals, m.p. > 300 °C, yield (73%). ^{1}H NMR (DMSO-d_6, 400 MHz) δ 6.09 (2H, *s*, CH_2), 6.84 (2H, *t*, ArH), 7.30–7.48 (16H, *m*, ArH + $2NH_2$), 7.85–7.99 (4H, *m*, ArH), 8.88 (2H, *s*, 2N=CH–), 9.12 (2H, *s*, 2NH), 12.65 (2H, *s*, 2NH). Anal. Calcd. (%) for $C_{35}H_{30}N_{10}O_4$ (654.68): C, 64.21; H, 4.62; N, 21.39. Found: C, 64.10; H, 4.70; N, 21.45%.

5,5′-(4,4′-Methylenebis(oxy)*bis*(benzylideneamino))*bis*(3-(4-methoxyphenylamino)-*N*-phenyl-1*H*-pyrazole-4-carboxamide) (18) Orange crystals, m.p. 250 °C, yield (76%). ^{1}H NMR (DMSO-d_6, 400 MHz, δ ppm) 3.73 (6H, *s*, $2OCH_3$), 6.14 (2H, *s*, CH_2), 6.91 (4H, *m*, ArH), 7.08 (2H, *t*, ArH), 7.35–7.41 (12H, *m*, ArH), 7.68 (4H, *d*, *J* = 7.8 Hz, ArH), 8.08 (4H, *d*, *J* = 8.1 Hz, ArH), 8.72 (2H, *s*, 2–N=CH–), 9.04 (2H, *s*, 2NH), 9.85 (2H, *s*, 2NH), 12.48 (2H, *s*, 2NH). Anal. Calcd. (%) for $C_{49}H_{42}N_{10}O_6$ (866.92): C, 67.89; H, 4.88; N, 16.16. Found: C, 67.80; H, 4.95; N, 16.10%.

5,5′-(4,4′-Methylenebis(oxy)*bis*(benzylideneamino))*bis*(3-(4-methoxyphenylamino)-*N*-(4-methylphenyl)-1*H*-pyrazole-4-carboxamide) (19) Yellow crystals, m.p. 266 °C, yield (81%). ^{1}H NMR (DMSO-d_6, 400 MHz, δ ppm): 2.27 (6H, *s*, $2CH_3$), 3.73 (6H, *s*, $2OCH_3$), 6.15 (2H, *s*, CH_2), 6.91 (4H, *s*, ArH), 7.15 (4H, *d*, *J* = 8.1 Hz, ArH), 7.32–7.57 (12H, *m*, ArH), 8.07 (4H, *d*, *J* = 8.1 Hz, ArH), 8.73 (2H, *s*, 2–N=CH–), 8.93 (2H, *s*, 2NH), 9.91 (2H, *s*, 2NH), 12.47

(2H, *s*, 2NH). Anal. Calcd. (%) for $C_{51}H_{46}N_{10}O_6$ (894.97): C, 68.44; H, 5.18; N, 15.65. Found: C, 68.35; H, 5.24; N, 15.71%.

5,5′-(4,4′-Methylene*bis*(oxy)*bis*(benzylideneamino))*bis*(3-(4-methoxyphenylamino)-*N*-(4-chlorophenyl)-1*H*-pyrazole-4-carboxamide) (20) Yellow crystals, m.p. 262 °C, yield (80%). IR (KBr) ν_{max}/cm^{-1} 3432, 3270 (NH), 1654 (C=O). ^{1}H NMR (DMSO-d_6, 400 MHz, δ ppm): 3.73 (6H, *s*, $2OCH_3$), 6.14 (2H, *s*, CH_2), 6.90 (4H, *d*, $J=8.6$ Hz, ArH), 7.31–7.42 (12H, *m*, ArH), 7.70 (4H, *d*, $J=8.8$ Hz, ArH), 8.07 (4H, *d*, $J=8.6$ Hz, ArH), 8.66 (2H, *s*, 2–N=CH–), 8.99 (2H, *s*, 2NH), 9.99 (2H, *s*, 2NH), 12.64 (2H, *s*, 2NH). ^{13}C NMR (DMSO-d_6, 100 MHz, δ ppm): 55.72 (2C, $2OCH_3$), 89.74 (3C, $1CH_2$ and $2C_4$-pyrazole), 114.97, 116.84, 117.29, 118.33, 121.24, 121.83, 128.90, 129.40, 131.88, 132.28, 138.42, 149.34 (34C, Ar), 153.84 ($2C_5$, pyrazole), 155.07 ($2C_3$, pyrazole), 158.30 (2C, 2–N=CH–), 160.47 (2C, Ar), 162.74 (2C=O). Anal. Calcd. (%) for $C_{49}H_{40}Cl_2N_{10}O_6$ (935.81): C, 62.89; H, 4.31; N, 14.97. Found: C, 62.95; H, 4.26; N, 14.92%.

5,5′-(4,4′-Ethylenebis(oxy)*bis*(benzylideneamino))*bis*(3-(phenylamino)-1*H*-pyrazole-4-carboxamide) (21) Yellow crystals, m.p. > 300 °C, yield (77%). ^{1}H NMR (DMSO-d_6, 400 MHz, δ ppm): 4.43 (4H, *s*, $2CH_2$), 6.86 (2H, *t*, ArH), 7.20 (4H, *d*, $J=8.1$ Hz, ArH), 2.27 (4H, *t*, ArH), 7.34, 7.39 (4H, 2*s*, $2NH_2$), 7.49 (4H, *d*, $J=7.7$ Hz, ArH), 7.97 (4H, *d*, $J=7.8$ Hz, ArH), 8.88 (2H, *s*, 2N=CH–), 9.12 (2H, *s*, 2NH), 12.21 (2H, *s*, 2NH). Anal. Calcd. (%) for $C_{36}H_{32}N_{10}O_4$ (668.70): C, 64.66; H, 4.82; O, 9.57. Found: C, 64.72; H, 4.76; O, 9.62%.

5,5′-(4,4′-Ethylenebis(oxy)*bis*(benzylideneamino))*bis*(3-(4-methoxyphenylamino)-*N*-phenyl-1*H*-pyrazole-4-carboxamide) (22) Yellow crystals, m.p. > 300 °C, yield (80%). IR (KBr) ν_{max}/cm^{-1} 3427, 3268 (NH), 1652 (C=O). ^{1}H NMR (DMSO-d_6, 400 MHz, δ ppm): 3.74 (6H, *s*, $2OCH_3$), 4.50 (4H, *s*, $2CH_2$), 6.90 (4H, *d*, $J=8.4$ Hz, ArH), 7.08 (2H, *t*, ArH), 7.20 (2H, *d*, $J=8.6$ Hz, ArH), 7.28 (4H, *d*, $J=8.3$ Hz, ArH), 7.37 (4H, *t*, ArH), 7.67 (4H, *d*, $J=8.2$ Hz, ArH), 7.89 (2H, *d*, $J=8.6$ Hz, ArH), 8.05 (4H, *d*, $J=8.3$ Hz, ArH), 8.71 (2H, *s*, 2–N=CH–), 8.98 (2H, *s*, 2NH), 9.98 (2H, *s*, 2NH), 12.61 (2H, *s*, 2NH). ^{13}C NMR (DMSO-d_6, 100 MHz, δ ppm): 55.29 (2C, $2OCH_3$), 66.78 (2C, $2CH_2$), 90.21 ($2C_4$, pyrazole), 115.08, 117.60, 121.44, 123.37, 127.44, 129.16, 129.91, 131.89, 132.78, 135.64, 138.53, 150.79 (34C, Ar), 153.52 ($2C_5$, pyrazole), 155.39 ($2C_3$, pyrazole), 156.33 (2C, 2–N=CH–), 162.51 (2C, Ar), 162.98 (2C=O). Anal. Calcd. (%) for $C_{50}H_{44}N_{10}O_6$ (880.95): C, 68.17; H, 5.03; N, 15.90. Found: C, 68.10; H, 5.09; N, 15.95%.

5,5′-(4,4′-Ethylenebis(oxy)*bis*(benzylideneamino))*bis*(3-(4-methoxyphenylamino)-*N*-(4-methylphenyl)-1*H*-pyrazole-4-carboxamide) (23) Yellow crystals, m.p. > 300 °C, yield (68%). ^{1}H NMR (DMSO-d_6, 400 MHz, δ ppm): 2.27 (6H, *s*, $2CH_3$), 3.72 (6H, *s*, $2OCH_3$), 4.52 (4H, *s*, $2CH_2$), 6.90 (4H, *d*, $J=6.6$ Hz, ArH), 7.16–7.28 (12H, *m*, ArH), 7.55 (4H, *d*, $J=7.8$ Hz, ArH), 8.04 (4H, *d*, $J=6.4$ Hz, ArH), 8.72 (2H, *s*, 2–N=CH–), 8.93 (2H, *s*, 2NH), 9.88 (2H, *s*, 2NH), 12.60 (2H, *s*, 2NH). Anal. Calcd. (%) for $C_{52}H_{48}N_{10}O_6$ (909.00): C, 68.71; H, 5.32; N, 15.41. Found: C, 68.62; H, 5.40; N, 15.35%.

5,5′-(4,4′-Ethylenebis(oxy)*bis*(benzylideneamino))*bis*(3-(4-methoxyphenylamino)-*N*-(4-chlorophenyl)-1*H*-pyrazole-4-carboxamide) (24) Yellow crystals, m.p. 282 °C, yield (74%). IR (KBr) ν_{max}/cm^{-1} 3426, 3272 (NH), 1656 (C=O). ^{1}H NMR (DMSO-d_6, 400 MHz, δ ppm): 3.72 (6H, *s*, $2OCH_3$), 4.50 (4H, *s*, $2CH_2$), 6.90 (4H, *d*, $J=8.1$ Hz, ArH), 7.18–7.26 (6H, *m*, ArH), 7.41 (4H, *d*, $J=8.6$ Hz, ArH), 7.69 (4H, *d*, $J=8.6$ Hz, ArH), 7.88 (2H, *d*, $J=8.6$ Hz, ArH), 8.04 (4H, *d*, $J=8.2$ Hz, ArH), 8.66 (2H, *s*, 2–N=CH–), 8.96 (2H, *s*, 2NH), 9.88 (2H, *s*, 2NH), 12.63 (2H, *s*, 2NH). ^{13}C NMR (DMSO-d_6, 100 MHz, δ ppm): 55.24 (2C, $2OCH_3$), 66.71 (2C, $2CH_2$), 93.51 ($2C_4$, pyrazole), 114.41, 115.47, 120.57, 128.92, 129.88, 131.42, 133.24, 137.50, 151.86 (34C, Ar), 153.10 ($2C_5$, pyrazole), 155.27 ($2C_3$, pyrazole), 156.52 (2C, 2–N=CH–), 162.33 (2C, Ar), 162.83 (2C=O). Anal. Calcd. (%) for $C_{50}H_{42}Cl_2N_{10}O_6$ (949.84): C, 63.23; H, 4.46; N, 14.75. Found: C, 63.14; H, 4.51; N, 14.69%.

Biological evaluation

In vitro cytotoxicity activity

Cell culture of HepG2 (human liver carcinoma), RPE-1 (human normal retina pigmented epithelium) and MCF-7 (human breast adenocarcinoma) cell lines was purchased from the American Type Culture Collection (Rockville, MD) and maintained in DMEM medium which was supplemented with 10% heat-inactivated fetal bovine serum (FBS), 100 U/ml penicillin and 100 U/ml streptomycin. The cells were grown at 37 °C in a humidified atmosphere of 5% CO_2.

MTT cytotoxicity assay

The cytotoxicity activities against HepG2, RPE-1 and MCF-7 human cell lines were estimated using the 3-[4,5-dimethyl-2-thiazolyl)-2,5-diphenyl-2*H*-tetrazolium bromide (MTT) assay, which is based on the cleavage of the tetrazolium salt by mitochondrial dehydrogenases in viable cells [41–44]. Cells were dispensed in a 96-well sterile microplate (5×10^4 cells/well) and incubated at 37 °C with series of different concentrations, in DMSO, of each

tested compound or Doxorubicin® (positive control) for 48 h in a serum-free medium prior to the MTT assay. After incubation, media were carefully removed, and 40 µL of MTT (2.5 mg/mL) was added to each well and then incubated for an additional 4 h. The purple formazan dye crystals were solubilized by the addition of 200 µL of DMSO. The absorbance was measured at 570 nm using a SpectraMax® Paradigm® Multi-Mode microplate reader. The relative cell viability was expressed as the mean percentage of viable cells compared to the untreated control cells. All experiments were conducted in triplicate and repeated in three different days. All the values were represented as mean ± SD. IC_{50}s were determined by probit analysis using SPSS software program (SPSS Inc., Chicago, IL).

Absorbance spectra

Absorbance spectra were measured on a Jenway UV–visible spectrophotometer, model 6505 (London, UK) using quartz cells of 1.00 cm path length. The UV–Vis absorbance spectra were recorded in the 200–500 nm range and spectral bandwidth of 3.0 nm. For the final spectrum of each solution analyzed, baseline subtraction of the buffer solution was performed. Genomic DNA was used in a concentration of 75 µg/ml. DNA was extracted from peripheral lymphocytes of anticoagulated blood (EDTA) samples by proteinase K digestion and phenol/chloroform extraction [53]. The purity was determined by measuring the absorbance at 260/280 nm indicating that the sample is free from protein contamination [53]. The concentration was assayed spectrophotometrically using 6600 M^{-1} cm^{-1} as a molar extinction coefficient at 260 nm.

Screening on thymidine phosphorylase

Enzyme rate spectral scans, studies of stoichiometric inhibition and absorbance readings at fixed wavelengths were conducted using a Jenway UV–visible spectrophotometer, model 6505 (London, UK) using quartz cells of 1.00 cm path length. T. Assays used thymidine as a substrate. The assay mixture contained (in 1 ml) 20 mM thymidine, 0.1 M potassium phosphate (pH 7.4) and limiting amounts of human TP (ca.0.00177 units per assay). The reaction was initiated by addition of enzyme, and the change in absorbance was monitored at 265 nm at 25 °C. Reaction enzyme kinetics data were analyzed using Grafit version 3 software (Erithacus software).

DNA binding properties

To study how competently the synthesized compounds interact with G-DNA, we investigated their DNA binding ability using fluorescence emission spectra. All experiments were conducted in *Tris* buffer (0.01 M Tris, 0.1 M NaCl, at pH 7.4). Glass-distilled deionized water and analytical-grade reagents were used throughout experiments. pH values of solutions were measured with a calibrated Jenway pH meter model 3510 (Staffordshire, UK). All buffer solutions were filtered through Millipore filters (Millipore, UK) of 0.45 mm pore diameter.

Fluorescence spectra and DNA binding studies

Fluorescence emission and excitation spectra were measured using a Jasco FP-6200 spectrofluorometer (Tokyo, Japan) using fluorescence four-sided quartz *cuvettes* of 1.00 cm path length. The automatic shutter-on function was used to minimize photo-bleaching of the sample. The selected excitation wavelength for ethidium bromide was 480 nm. The emission spectrum was corrected for background fluorescence of the buffer. The ethidium bromide (EB) fluorescence displacement experiment was performed by sequential addition of aliquots of 1790 µl Tris buffer, 10 µl EB (final concentration of 72 µM), 100 µl G-DNA from stock solutions (1.5 mg/ml) and finally 10 µl of the compounds, final concentration of 30 µM. Emission spectra were recorded for each system using excitation wavelengths of maximum fluorescence intensity determined for the systems to be 480 nm using a slit width of 5 nm to examine alterations in emission spectra resulting from the complex construction of both systems. On construction of the full systems, the system was allowed to equilibrate for 30 min at room a temperature and emission spectra (500–730 nm) were recorded to monitor changes in EB intensity. Ethidium bromide displacements IC_{50} was determined, in which the IC_{50} values are the concentration of the tested substances required to decrease the fluorescence of the ethidium bromide–DNA complex by 50% [54].

Binding energy

The molecular docking simulation method is primarily validated on the basis of the obtained binding energy. The predefined range of binding energy is supposed to be in the range between − 5 and − 15 kcal/mol to productively validate the molecular docking process.

Molecular docking study

MGL (Molecular Graphics Laboratory) tools 1.5.4 with AutoDock 4 and AutoGrid 4.0 were used to set up and exert blind docking calculations between our derivatives and DNA sequences. DNA sequences:

DNA (5′-D(*CP*GP*CP*GP*AP*AP*TP*TP*CP*GP*CP*G)-3′) (PDB ID: **1bna**),

DNA (5′-D(*CP*GP*CP*AP*AP*AP*TP*TP*TP*GP*CP*G)-3′) (PDB ID: **102d**), DNA (5′-D(*CP*GP*TP*AP*CP*G)-3′) (PDB ID: **1k2j**), DNA (5′-D(*CP*GP*CP*GP*AP*AP*TP*TP*CP*GP*CP*G)-3′) (PDB ID: **2gvr**) and DNA (5′-D(*CP*GP*TP*AP*CP*G)-3′) (PDB ID: **2des**), were obtained from the Protein Data Bank and were used for the docking studies. *Bis*-Schiff bases of pyrazoles **9–24** structures were drawn and optimized using ChemDraw Ultra (version 8.0, Cambridge soft Com., USA). Chem3D Ultra was used to convert 2D into 3D structures, and the energy was minimized using the semiempirical AM1 method which is based on the neglect of differential diatomic overlap (NDDO) integral approximation. The molecular dockings of *Bis*-Schiff bases of pyrazole **9–24** with B-DNAs (B: right-handed double-helix DNA) were accomplished by AutoDock 4.2 software from the Scripps Research Institute (TSRI) (http://autodock.scripps.edu/). Firstly, the polar hydrogen atoms were added into B-DNA molecules. Then, the partial atomic charges of the B-DNA and *Bis*-Schiff bases of pyrazole **9–24** were calculated using Kollman methods [55]. In the process of molecular docking, the grid maps of dimensions (62 Å×62 Å×62 Å) with a grid-point spacing of 0.376 Å and the grid boxes centered. The number of genetic algorithm runs and the number of evaluations were set to 100. All other parameters were default settings. Cluster analysis was performed on docking results by using a root mean square (RMS) tolerance of 2.0 Å, dependent on the binding free energy. Lastly, the dominating configuration of the binding complex of our compounds and B-DNA fragments with minimum binding energy can be determined.

Acknowledgements Authors thank National Research Centre for the financial support through scientific project number 12010103.

Compliance with ethical standards

Conflict of interest The authors declare that they have no conflict of interest.

References

1. P. Majumder, S.K. Pradhan, P.G. Devi, S. Pal, D. Dasgupta, Subcell. Biochem. **41**, 145–189 (2007)
2. J.A. Hartley, D. Hochhauser, Curr. Opin. Pharmacol. **12**, 398–402 (2012)
3. A. Srinivasan, B. Gold, Future Med. Chem. **4**, 1093–1111 (2012)
4. C.R. Prakash, S. Raja, J. Saudi Chem. Soc. **17**, 337–344 (2011)
5. H.D. Revanasiddappa, K.S. Prasad, L.S. Kumar, B. Jayalakshmi, Int. J. ChemTech Res. **2**, 1344–1349 (2010)
6. K.S. Kumar, S. Ganguly, R. Veerasamy, E.D. Clercq, Eur. J. Med. Chem. **45**, 5474–5479 (2010)
7. X. Zhou, L. Shao, Z. Jin, J.-B. Liu, H. Dai, J.-X. Fang, Heteroat. Chem. **18**, 55–59 (2007)
8. A.S. Hassan, T.S. Hafez, M.M. Ali, T.K. Khatab, Res. J. Pharm. Biol. Chem. Sci. **7**, 417–429 (2016)
9. G. Ouyang, Z. Chen, X.-J. Cai, B.-A. Song, P.S. Bhadury, S. Yang, L.-H. Jin, W. Xue, D.-Y. Hu, S. Zeng, Bioorg. Med. Chem. **16**, 9699–9707 (2008)
10. E.M. Sharshira, N.M.M. Hamada, Molecules **17**, 4962–4971 (2012)
11. S. Bondock, S. Adel, H.A. Etman, F.A. Badria, Eur. J. Med. Chem. **48**, 192–199 (2012)
12. S. Malladi, A.M. Isloor, S. Isloor, D.S. Akhila, H.-K. Fun, Arab. J. Chem. **6**, 335–340 (2013)
13. X.-H. Lv, Z.-L. Ren, D.-D. Li, B.-F. Ruan, Q.-S. Li, M.-J. Chu, C.-Y. Ai, D.-H. Liu, K. Mo, H.-Q. Cao, Chin. Chem. Lett. **28**, 377–382 (2017)
14. A. Jarrahpour, D. Khalili, E.D. Clercq, C. Salmi, J.M. Brunel, Molecules **12**, 1720–1730 (2007)
15. A.S. Hassan, A.A. Askar, A.M. Naglah, A.A. Almehizia, A. Ragab, Molecules **25**, 2593 (2020)
16. M.A. Elsherif, A.S. Hassan, G.O. Moustafa, H.M. Awad, N.M. Morsy, J. Appl. Pharm. Sci. **10**, 37–43 (2020)
17. A.S. Al-Wasidi, A.S. Hassan, A.M. Naglah, J. Appl. Pharm. Sci. **10**, 142–148 (2020)
18. A.M. Naglah, A.A. Askar, A.S. Hassan, T.K. Khatab, M.A. Al-Omar, M.A. Bhat, Molecules **25**, 1431 (2020)
19. A.S. Hassan, A.A. Askar, E.S. Nossier, A.M. Naglah, G.O. Moustafa, M.A. Al-Omar, Molecules **24**, 3130 (2019)
20. T.K. Khatab, A.S. Hassan, T.S. Hafez, Bull. Chem. Soc. Ethiop. **33**, 135–142 (2019)
21. A.S. Hassan, G.O. Moustafa, A.A. Askar, A.M. Naglah, M.A. Al-Omar, Synth. Commun. **48**, 2761–2772 (2018)
22. A.A. Magd-El-Din, H.A. Mousa, A.A. Labib, A.S. Hassan, A.S. Abd El-All, M.M. Ali, A.A. El-Rashedy, A.H. El-Desoky, Z. Naturforsch. C **73**, 465–478 (2018)
23. H.R. Elgiushy, S.F. Hammad, A.S. Hassan, N. Aboutaleb, K.A.M. Abouzid, J. Adv. Pharm. Res. **4**, 221–237 (2018). https://doi.org/10.21608/aprh.2018.2839.1049
24. A.S. Hassan, T.S. Hafez, J. Appl. Pharm. Sci. **8**, 156–165 (2018)
25. M. El-Naggar, A.S. Hassan, H.M. Awad, M.F. Mady, Molecules **23**, 1249 (2018)
26. A.S. Hassan, H.M. Awad, A.A. Magd-El-Din, T.S. Hafez, Med. Chem. Res. **27**, 915–927 (2018)
27. A.S. Hassan, G.O. Moustafa, H.M. Awad, Synth. Commun. **47**, 1963–1972 (2017)
28. A.S. Hassan, D.M. Masoud, F.M. Sroor, A.A. Askar, Med. Chem. Res. **26**, 2909–2919 (2017)
29. A.S. Abd El-All, A.S. Hassan, S.A. Osman, H.A.A. Yosef, W.H. Abdel-Hady, M.A. El-Hashash, S.R. Atta-Allah, M.M. Ali, A.A. El-Rashedy, Acta Pol. Pharm. **73**, 79–92 (2016)
30. A.S. Hassan, T.S. Hafez, S.A. Osman, M.M. Ali, Turk. J. Chem. **39**, 1102–1113 (2015)
31. A.S. Hassan, S.A. Osman, T.S. Hafez, Egypt. J. Chem. **58**, 113–139 (2015)
32. S.A. Osman, H.A. Mousa, H.A.A. Yosef, T.S. Hafez, A.A. El-Sawy, M.M. Abdallah, A.S. Hassan, J. Serb. Chem. Soc. **79**, 953–964 (2014)
33. T.S. Hafez, S.A. Osman, H.A.A. Yosef, A.S. Abd El-All, A.S. Hassan, A.A. El-Sawy, M.M. Abdallah, M. Youns, Sci. Pharm. **81**, 339–357 (2013)
34. S.A. Osman, H.A.A. Yosef, T.S. Hafez, A.A. El-Sawy, H.A. Mousa, A.S. Hassan, Aust. J. Basic Appl. Sci. **6**, 852–863 (2012)
35. G.H. Elgemeie, S.H. Elsayed, A.S. Hassan, Synth. Commun. **39**, 1781–1792 (2009)

36. G.H. Elgemeie, S.H. Elsayed, A.S. Hassan, Synth. Commun. **38**, 2700–2706 (2008)
37. A.S. Hassan, T.S. Hafez, S.A. Osman, Sci. Pharm. **83**, 27–39 (2015)
38. H.R. Darabi, A.R. Mohebbi, M. Bolourtchian, Supramol. Chem. **15**, 465–468 (2003). https://doi.org/10.1080/1061027031000159919 5
39. A. Ali, J. Merza, Inorg. Chem. Ind. J. **12**, 111 (2017)
40. M. Hajibeygi, M. Shabanian, Chin. J. Polym. Sci. **32**, 758–767 (2014). https://doi.org/10.1007/s10118-014-1449-2
41. S.F. Mohamed, E.R. Kotb, E.A. Abd El-Meguid, H.M. Awad, Res Chem Intermed **43**, 437–456 (2017). https://doi.org/10.1007/s11164-016-2633-5)
42. E.M. Flefel, W.A. El-Sayed, A.M. Mohamed, W.I. El-Sofany, H.M. Awad, Molecules **22**, 170 (2017). https://doi.org/10.3390/molecules22010170
43. H.M. Awad, H.I. Abd-Alla, K.H. Mahmoud, S.A. El-Toumy, Med. Chem. Res. **23**, 3298–3307 (2014)
44. A.S. Hassan, M.F. Mady, H.M. Awad, T.S. Hafez, Chin. Chem. Lett. **28**, 388–393 (2017). https://doi.org/10.1016/j.cclet.2016.10.022
45. P.A. Holt, J.B. Chaires, J.O. Trent, J. Chem. Inf. Model. **48**, 1602–1615 (2008)
46. Y. Gilad, H. Senderowitz, J. Chem. Inf. Model. **54**, 96–107 (2014)
47. A.J. Hampshire, K.R. Fox, Biochimie **90**, 988–998 (2008)
48. M.J. Waring, Drugs Exp. Clin. Res. **12**, 441–453 (1986)
49. A.A. Hassan, A.A. Aly, N.K. Mohamed, K.M. El Shaieb, M.M. Makhlouf, E.M.N. Abdelhafez, S. Brase, M. Nieger, K.N. Dalby, T.S. Kaoud, Bioorg. Chem. **85**, 585–599 (2019)
50. S. Mohan, S. Rangappa, N.C. Anilkumar, J.E. Fuchs, A. Bender, K.S. Rangappa, R. Bhatnagar, Chem. Biodivers. **16**, e1800435 (2019). https://doi.org/10.1002/cbdv.201800435
51. E.K. Carter, S. Laughlin-Toth, T. Dodd, W.D. Wilson, I. Ivanov, Phys. Chem. Chem. Phys. **21**, 1841–1851 (2019). https://doi.org/10.1039/c8cp05537h
52. S.N. Ho, S.H. Boyer, S.L. Schreiber, S.J. Danishefsky, G.R. Crabtree, Proc. Natl. Acad. Sci. U. S. A. **91**, 9203–9207 (1994)
53. M.B. Johns, J.E. Paulus-Thomas, Anal. Biochem. **180**, 276–278 (1989). https://doi.org/10.1016/0003-2697(89)90430-2
54. M.B. Smuckler, L. Guan, A. Nakanishi, H. Kasamatsu, M.F. Hawthorne, in *Frontiers in Neutron Capture Therapy*, ed. by M.F. Hawthorne, K. Shelly, R.J. Wiersema (Springer, Boston, 2001), p. 1117
55. R. Tiwari, K. Mahasenan, R. Pavlovicz, C. Li, W. Tjarks, J. Chem. Inf. Model. **49**, 1581–1589 (2009)